

# State Representation Learning from Demonstration

Astrid Merckling<sup>1</sup>, Alexandre Coninx<sup>1</sup>, Loic Cressot<sup>1</sup>, Stephane Doncieux<sup>1</sup> and Nicolas Perrin<sup>1</sup>

**Abstract**—In a context where several policies can be observed as black boxes on different instances of a control task, we propose a method to derive a state representation that can be relied on to reproduce any of the observed policies. We do so via imitation learning on a multi-head neural network consisting of a first part that outputs a common state representation and then one head per policy to imitate. If the demonstrations contain enough diversity, the state representation is general and can be transferred to learn new instances of the task. We present a proof of concept with experimental results on a simulated 2D robotic arm performing a reaching task, with noisy image inputs containing a distractor, and show that the state representations learned provide a greater speed up to end-to-end reinforcement learning on new instances of the task than with other classical representations.

## I. INTRODUCTION

While robotic simulation setups could provide the robot’s state directly to the learning algorithm, there are many other setups where this is not the case and no simple state representation summarizing all task-relevant information can be assumed. To give a concrete example, imagine a set of robotic tasks that can be considered either in *laboratory* conditions, where the sensory input is rich and precise (e.g. motion capture), or in *real-world* conditions, where the sensory input is more complex and less reliable (e.g. embedded cameras). Designing controllers may be relatively easy in *laboratory* conditions, and much harder in *real-world* conditions. For example, drone control is much easier when motion capture is available, but for *real-world* use, controllers cannot assume that motion capture is available. We therefore believe that learning directly from robot perceptions without assuming that the robot state is available is a desirable goal. The controllers designed in *laboratory* conditions can be used to generate demonstrations on various instances of the control task. The principle of the method introduced in this paper is to attempt to imitate the behavior of these demonstration controllers without resorting to the *laboratory* sensory input. Our approach attempts to construct a single state representation that depends only on the *real-world* sensory input and that could potentially be used to reproduce all the demonstrated tasks. Hopefully, the state representation learned can then be exploited to learn more efficiently new instances of the control task in *real-world* conditions. We do not address an example of *laboratory* conditions vs. *real-world* conditions experiments in this paper, but it illustrates the motivation of our approach.

It is known that data representation has an important impact on the performance of machine learning algorithms. Well-

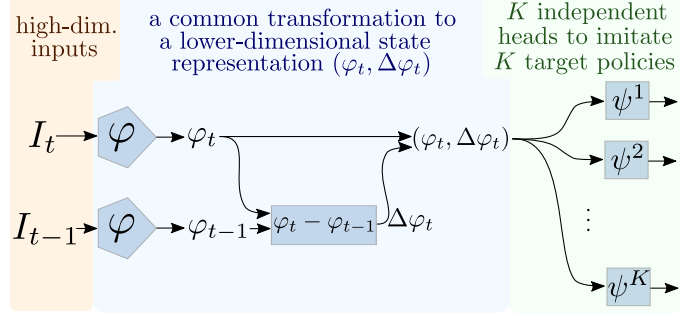


Fig. 1. Neural network architecture for the proposed state representation learning from demonstration method. High-dimensional inputs (e.g. raw images) are transformed into more compact representations via the network  $\varphi$ . From the representations  $\varphi_{t-1}$  and  $\varphi_t$  of two consecutive inputs  $I_{t-1}$  and  $I_t$ , a state representation  $(\varphi_t, \Delta\varphi_t)$  (with  $\Delta\varphi_t = \varphi_t - \varphi_{t-1}$ ) is computed and sent to the multiple heads  $\psi^i$ . Each head is used to reproduce one of the observed target policies.

thought feature engineering can often make the difference between the failure or success of a learning process. In their review of representation learning, Bengio et al. [1] formulate the hypothesis that the most relevant pieces of information contained in the data can be more or less entangled and hidden in different representations. If a representation is adequate, functions that map inputs to desired outputs are somewhat less complex and thus easier to construct via learning. However, a frequent issue is that these adequate representations may be difficult to design, and this is true in particular when the raw data consists of images, i.e. 2D arrays of pixels. One of the objectives of deep learning methods is to automatize feature extraction so as to make learning algorithms effective even on raw data. By composing multiple non-linear transformations, the neural networks on which these methods rely are capable of progressively creating more abstract and useful representations of the data in their successive layers (Olah et al. [2] illustrate some of these mechanisms).

The features within a neural network are typically acquired via training on a learning task, such as classification of some data into different categories. As a result a portion of these features tend to be very specific to the learning task. Yet, if the input data exhibit enough diversity, some of the learned features will also be general, which makes them potentially useful for other learning tasks. This is the principle of transfer learning [3]: after training a base network on a base dataset and task, learned features are then integrated in a network that will be trained on another task (or a different instance of the same task). If the features are general, they are likely to accelerate the learning process.

In this paper, we are interested in solving robotic control tasks via end-to-end reinforcement learning (RL), using raw

<sup>1</sup>Sorbonne Université, CNRS, Institut des Systèmes Intelligents et de Robotique, ISIR, F-75005 Paris, France, Email: {astrid.merckling, alexandre.coninx, stephane.doncieux, nicolas.perrin}@sorbonne-universite.fr

images as inputs, without having access to any other sensor, which means in particular that the robot configuration is a priori unknown (in the illustrative example we consider for experimental evaluation, we do not give access to the joint angles and angular velocities of a 2D robot arm). We assume that at all time the high-dimensional observations  $I_t$  (the images) contain enough information to know the robot configuration  $\mathbf{q}_t$ , and that the controller only needs to rely on this configuration and its velocity,  $\dot{\mathbf{q}}_t$ , to choose actions. Intuitively, the state  $\mathbf{s}_t = (\mathbf{q}_t, \dot{\mathbf{q}}_t)$ , which we will call *ground truth state* in the remainder of the paper, could probably be a much better input for a RL algorithm than the raw images, but without prior knowledge it is not easy to get  $\mathbf{q}_t$  from  $I_t$ . In robotics, state representation learning [4] aims at constructing a mapping from high-dimensional observations to lower-dimensional and denser representations that, similarly to  $\mathbf{s}_t$ , can be advantageously used instead of  $I_t$  to form the inputs of a controller. Several works have shown that using learned state representations can accelerate image-based RL. In an approach proposed by Finn et al. [5], the robot configuration is known, but the considered tasks depend on object positions and orientations that can only be inferred from camera images. Deep spatial autoencoders are used to learn a state representation that consists of feature points in the image. This enables more efficient RL for manipulation tasks than a previous work by Levine et al. [6] in which end-to-end learning was performed without acquiring a low-dimensional representation first. In another approach proposed by Jonschkowski & Brock [7], the state representation learning is formulated as an optimization problem over several costs expressing robotic priors, i.e. properties that can be expected from a state representation in robotics. Using the state representations learned by this method instead of raw visual observations improves efficiency and generalization in RL.

We consider a context in which demonstrations are available: an agent can observe several successful policies on various instances of a task. The goal of this paper is to show that such observations can be useful to learn state representations that are particularly appropriate for control. Indeed, demonstrations are made with policies that exploit structured inputs (full knowledge of the system state) ; but it is often useful to try learning similar tasks using deteriorated inputs (cf. the drone example mentioned above). The literature in imitation learning [8] has shown that demonstrations can be very valuable to learn new policies, or to extract the most relevant features of a pre-defined feature representation [9], [10]. To the best of our knowledge no previous work has focused on constructing reusable state representations from raw inputs solely from demonstrations, so we believe that it can be interesting for transfer learning. Indeed, if by imitating several demonstrations on various instances of a task, we can construct a unique state representation that is adequate for all of them, then it is likely to be a quite general representation, potentially very useful to subsequently bootstrap the learning process on new instances of the task. It is the diversity in the demonstrations that forces the state representation to be general. Figure 1 summarizes the proposed method. This method, which we call State Representation

Learning from Demonstration (SRLfD), is presented in more details in Section III, after an overview of the existing related work in Section II.

In Sections IV and V, we describe our experimental setup and results with a simulated 2D robotic arm on various instances of a reaching task. Once the imitation learning stage is done, to validate the usefulness of the learned state representation, we define new instances of the task and train new heads  $\psi$  via RL (using the popular DDPG algorithm [11]). We show that using the state representation instead of raw images can significantly accelerate RL. When the state representation is chosen to be low-dimensional, the speed up brought by our method is greater than the one resulting from state representations obtained with deep autoencoders, or with principal component analysis (PCA).

## II. RELATED WORK

State representation learning (SRL) for control is the idea of extracting from the sensory stream the information that is relevant to control the robot and its environment and representing it in a way that is suited to drive robot actions. It has been subject to a lot of recent attention [4]. It was proposed as a way to overcome the curse of dimensionality, to speed up and improve RL, to achieve transfer learning, to ignore distractors, and to make artificial autonomous agents more transparent and explainable.

Since the curse of dimensionality is a major concern, many state representation techniques are based on dimension reduction [12] and classic unsupervised learning techniques such as principal component analysis (PCA) [13] or its non-linear version, the autoencoder [14]. Those techniques allow to compress the observation in a compact latent space, from which it can be reconstructed with minimal error. Further developments led to variational autoencoders (VAE) [15] and then their extension  $\beta$ -VAE [16], which are powerful generative models able to learn a disentangled representation of the observation data. However, the goal of those methods is to model the observation data; they do not take actions or rewards into account, and the representation they learn aims at allowing the minimization of a reconstruction loss, not at extracting the most relevant information for control. In particular, their behavior is independent from actions, rewards or the temporal structure of the observations, and they cannot discriminate distractors.

To overcome this limitation, a common approach to state representation is to couple an autoencoder to a forward model predicting the future state [17]. Most of those self-supervised approaches make the assumption that the forward model in the learned state space must be linear, although some can learn complex nonlinear dynamics [18]. Further developments have used spatial and temporal coherence to build an accurate environment representation [19].

A different approach to state representation is to forego observation reconstruction and to learn a representation satisfying some physics-based priors like temporal coherence, causality and repeatability [7] or controllability [20]. Those methods have been shown to learn representations able to speed up

RL, but this improvement is contingent on the careful choice and weighting of the priors suited to the task and environment. Similar ideas also led to time-contrastive networks [21], which use time as a supervisory signal to learn the structure present in videos and build a robust task-agnostic visual representation.

Learning state representations from demonstrations of multiple policies solving different tasks instances, as we propose, also has some similarities with multi-task RL [22] and transfer learning [23]. Multi-task learning aims to learn several similar but distinct tasks simultaneously to accelerate the learning or improve the quality of the learned policies, while transfer learning strives to exploit the knowledge of how to solve a given task to then improve the learning of a second task. Not all multi-task and transfer learning works rely on explicitly building a common representation, but some do, either by using a shared representation during multiple task learning [24] or by distilling a generic representation from task-specific features [25]. The common representation can then be used to learn new tasks. A similar idea is to use an auxiliary task to bootstrap learning for sparse and delayed rewards [26]: a self-supervised task allows the robot to explore and learn a representation, which is then used to solve the initial task. Some other approaches to multi-task learning use meta-learning to directly train a model-agnostic representation applicable to a family of tasks [27], or rely on a modular decomposition of a deep network into task modules and robot modules to build task-agnostic and robot-agnostic representations [28]. All those techniques do allow to build state representations in a sample-efficient way, but they rely on exploration of the task space and on-policy data collection, whereas we focus on situations where only a limited number of preexisting demonstrations from a given set of existing policies are available.

In another perspective, the learning from demonstrations literature typically focuses on learning from a few examples and generalizing from those demonstrations, for example by learning a parameterized policy using control-theoretic methods [29] or RL-based approaches [30]. Although those methods typically assume prior knowledge of a compact representation of the robot and environment, some of them directly learn and generalize from visual input [31] and do learn a state representation. However, the goal is not to reuse that representation to learn new skills but to produce end-to-end visuomotor policies generalizing the demonstrated behaviors in a given task space.

Several works have also proposed using demonstrations to improve regular deep RL techniques [32], [33], but the goal is mostly to improve exploration in environments with sparse rewards. Those works do not directly address the problem of state representation learning.

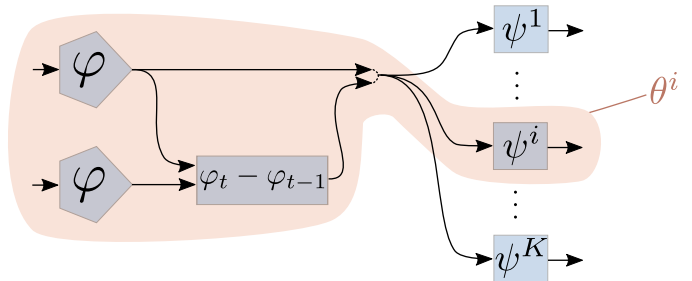


Fig. 2. Each head  $\psi^i$  defines a sub-network that contains the parameters of  $\varphi$  and the parameters of  $\psi^i$ . Together, they form the vector of parameters  $\theta^i$ .  $\theta$  is the vector of parameters of the whole network.

### III. LEARNING A STATE REPRESENTATION FROM DEMONSTRATIONS

#### A. Tasks

We consider a set of tasks or instances of tasks<sup>1</sup>  $T^i$ ,  $i \in \{1, 2, \dots, K\}$ , and for each of them a set of demonstrations that have been produced by a target policy  $\pi_{\text{target}}^i$ . Although these demonstrations consist of multiple observed trajectories, for example obtained by running the target policy from various initial conditions, we store them as a single set of triples  $\mathcal{D}^i = \{(I_{t-1}^i, I_t^i, \mathbf{a}_t^i)\}_t$ , where  $I_{t-1}^i$  and  $I_t^i$  are consecutive high-dimensional observations, and  $\mathbf{a}_t^i$  is a real-valued vector corresponding to the action executed right after the observation  $I_t^i$  was made. The policy  $\pi_{\text{target}}^i$  may have used additional sensory input to compute  $\mathbf{a}_t^i$ , but we assume that all the information needed to reproduce the output  $\mathbf{a}_t^i$  is contained in  $(I_{t-1}^i, I_t^i)$ .

#### B. Minimizing Action Prediction Error

Following the architecture described in Figure 1, we use a neural network  $\varphi$  that maps high-dimensional observations  $I_t^i$  to a smaller real-valued vector  $\varphi(I_t^i) = \varphi_t^i$ . Two copies of  $\varphi$  (i.e. neural networks with the same structure and shared weights) are applied to  $I_t^i$  and  $I_{t-1}^i$ . Their combined output is  $(\varphi_t^i, \varphi_{t-1}^i)$ , which we transform into  $(\varphi_t^i, \Delta\varphi_t^i)$ , with  $\Delta\varphi_t^i = \varphi_t^i - \varphi_{t-1}^i$ . We choose as a state representation  $(\varphi_t^i, \Delta\varphi_t^i)$  that is particularly suited for mechanical systems. The learned representation has somehow a physical meaning (a vector containing information about the robot state, and its derivative containing information about the robot velocity), but the transformation between it and the ground-truth state can nevertheless be complex. The state representation  $(\varphi_t^i, \Delta\varphi_t^i)$  is sent to  $K$  independent heads of our neural network architecture:  $\psi^1, \psi^2, \dots, \psi^K$ . The number of heads  $K$  corresponds to the number of different instances of the task for which demonstrations are available. Each head has continuous outputs with the same number of dimensions as the action space of the robot. We denote by  $\psi^i(\varphi_t^i, \Delta\varphi_t^i)$  the output of the  $i$ -th head of the network on the input  $(I_{t-1}^i, I_t^i)$ . We train the global network to imitate all the target policies via supervised learning in the following way. Let us

<sup>1</sup>Roughly, different tasks refer to objectives of different nature, while different instances of a task refer to a difference of parameters in the task. For example, reaching various locations with a robotic arm is considered as different instances of the same reaching task.

denote by  $\mathbb{E}_{\mathcal{D}^i}[\cdot]$  the averaging operator over the distribution of samples  $(I_{t-1}^i, I_t^i, \mathbf{a}_t^i)$  defined by  $\mathcal{D}^i$ . We also denote by  $\theta$  the vector of parameters of the global network, and by  $\theta^i$  the vector of parameters involved in the path to the output of head  $\psi^i$ , as shown in Figure 2. Our goal is to minimize the quantities  $\mathbb{E}_{\mathcal{D}^i} [\|\psi^i(\varphi_t^i, \Delta\varphi_t^i) - \mathbf{a}_t^i\|_2^2]$  that measure how well the target policies are imitated. These quantities depend on the parameters  $\theta^i$ , so we want to solve the  $K$  optimization problems

$$\arg \min_{\theta^i} \mathbb{E}_{\mathcal{D}^i} [\|\psi^i(\varphi_t^i, \Delta\varphi_t^i) - \mathbf{a}_t^i\|_2^2],$$

for  $i \in \{1, \dots, K\}$ . Of course, there is an interweaving between these optimization problems as their parameters are not independent: all the vectors  $\theta^i$  contain the parameters of  $\varphi$ . We give an equal importance to all target policies by iteratively picking a random  $i \in \{1, \dots, K\}$ , then a random batch of samples  $\mathcal{B}^i \subset \mathcal{D}^i$ , and performing a gradient descent step on  $\mathbb{E}_{\mathcal{B}^i} [\|\psi^i(\varphi_t^i, \Delta\varphi_t^i) - \mathbf{a}_t^i\|_2^2]$  to adjust  $\theta^i$ . Algorithm 1 describes this procedure. For efficiency purposes, our implementation differs slightly from the pseudo-code in that some gradient steps for different tasks  $T^i$  are computed in parallel.

The network of our SRLfD is trained to reproduce the demonstrations, but without direct access to the structured state. Each imitation can only be successful if the required information about the robot state is extracted by the state representation  $(\varphi_t^i, \Delta\varphi_t^i)$ . However, a single task may not require the knowledge of the full robot state. Hence, we cannot be sure that reproducing only one instance of task would yield a good state representation. By learning a common representation for various instances of tasks, we increase the probability that the learned representation is general and complete. It can then be used as a convenient input for downstream learning tasks, in particular end-to-end reinforcement learning.

#### IV. EXPERIMENTAL SETUP

The whole end-to-end reinforcement learning is challenging despite the simplicity of the task considered in this work. As the heart of our work concerns state representation extraction, we have focused on making perception challenging, by adding noise and distractors to the inputs. We believe that the complexity of the control part (i.e. the complexity of the tasks) is less important to validate our method, as it depends more on the performance of the reinforcement learning algorithm. To solve even just the simple reaching task, the information of the robot arm position, for instance, is required and needs to be extracted from the image for the RL algorithm to converge. Indeed our results show that this is the case when SRLfD compressed state representation is used as input of DDPG [11].

##### A. SRLfD Training Setup

**Environment:** We consider a simulated 2D robotic arm with 2 torque-controlled joints, as shown in Figure 3. It is the “reacher” environment from the Deepmind control suite [34] MuJoCo [35] benchmark on continuous control tasks. An instance of this task is parameterized by the position of a goal that the end-effector of the robot must reach within some margin of error (and in limited time). We use as raw inputs

#### Algorithm 1 SRLfD algorithm

**Input:**

- A set of instances of tasks  $T^i$ ,  $i \in \{1, \dots, K\}$ , and for each of them a set of demonstrations  $\mathcal{D}^i = \{(I_{t-1}^i, I_t^i, \mathbf{a}_t^i)\}_t$ .
- A randomly initialized neural network following the architecture described in Figure 1 with weights  $\theta$ .

**for**  $epoch = 1$  **to**  $M$  **do**

**for**  $step = 1$  **to**  $N$  **do**

    Pick randomly  $i \in \{1, \dots, K\}$ .

    Pick a random subset of samples to form a batch  $\mathcal{B}^i \subset \mathcal{D}^i$ .

    Adjust  $\theta$  with a gradient descent step on the following expression to minimize:

$$\mathbb{E}_{\mathcal{B}^i} [\|\psi^i(\varphi_t^i, \Delta\varphi_t^i) - \mathbf{a}_t^i\|_2^2].$$

**end for**

**end for**

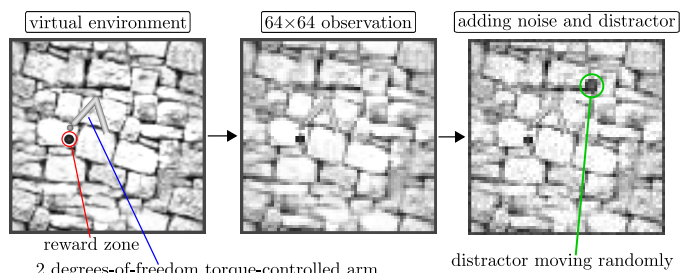


Fig. 3. The “reacher” environment, with a reward of 1 when the end-effector reaches a position close to the goal, and 0 otherwise.

grayscale images of  $64 \times 64$  pixels. To increase the difficulty of the learning, in some cases we add a randomly moving distractor and Gaussian noise, as shown on Figure 3.

**Generating demonstrations:** For simplicity, we allow the target policies to have access to the *ground truth state* of the robot  $(\mathbf{q}, \dot{\mathbf{q}})$ , where  $\mathbf{q}$  is the configuration of the robot arm, represented as a vector of size 4:  $(\cos \alpha_1, \sin \alpha_1, \cos \alpha_2, \sin \alpha_2)$ ,  $\alpha_1$  and  $\alpha_2$  being respectively the first and second joint angles in radians. To construct the target policies, we run the Hindsight Experience Replay (HER) RL algorithm [36] that also exploits the  $(x, y)$  parameters of the goal position. It returns a parameterized policy capable of producing reaching motions to any reachable goal position. Note that the purpose of our method is to generate state representation from (possibly noisy) inputs that are hard to exploit (such as raw images), so access to the robot state is only given to the target policies that generate demonstrations. The demonstration data used to train SRLfD consists of 16 different instances of the reaching task, with for each of them 262 trajectories computed from various initial positions using the target policy obtained with HER.

##### B. Quantitative Evaluation Setup

To quantitatively evaluate the usefulness of the state representation generated with our method, we run the RL algorithm DDPG [11] on a new instance of the reaching task, chosen

randomly, and compare the learning curve to the ones obtained with state representations originating from other methods. The performance of a policy is measured as the mean success rate, i.e. the probability to reach the reward (i.e. the goal) from a random initial configuration in 50 time steps or less. We expect that better representations yield faster learning progress (in average).

**Baseline Methods:** We compare state representations obtained with our method (SRLfD) to 4 other types of state representations:

- Ground truth: as mentioned in Section IV, what we call *ground truth* representation of the robot configuration is  $\mathbf{q} = (\cos \alpha_1, \sin \alpha_1, \cos \alpha_2, \sin \alpha_2)$ , where  $\alpha_1$  and  $\alpha_2$  are the joint angles in radians. The  $(\mathbf{q}, \dot{\mathbf{q}})$  representation is of size 8.
- Principal Component Analysis (PCA) [37]: we perform PCA on the demonstration data, and the 8 or 24<sup>2</sup> most significant dimensions are kept, thus reducing observations to a compact vector that accounts for a large part of the input variability. Note that the representation replaces  $\varphi$  in the architecture of Figure 1, so the full state representation  $(\varphi, \Delta\varphi)$  has twice as many dimensions as the number of dimensions chosen for the PCA.
- Autoencoder-based representation [14]:  $\varphi$  is replaced by a representation learned with an auto-encoder that has a symmetric structure, with transposed convolution layers [38] in its decoding part. The latent space representation of the autoencoder (of size 8 or 24) is trained with the same number of input samples from the demonstrations (but ignoring the actions) as in the SRLfD training. Again, the subsequent representation has twice the size of the latent space.
- Random network representation [39]: we use the same neural network structure for  $\varphi$  as with SRLfD, but instead of training its parameters, they are simply set to random values.

### C. Implementation Details

**SRLfD architecture:** The network  $\varphi$  (see Figure 1) sends its  $64 \times 64$  input to a succession of 3 convolution layers with 16 filters of size  $3 \times 3$ , each being followed by max-pooling with  $2 \times 2$  filters and stride 1. It ends with a fully connected layer with half as many output units as the chosen state representation dimension (because state representations have the form  $(\varphi, \Delta\varphi)$ ). The function  $x \mapsto 1.7159 \tanh(\frac{2}{3}x)$  is used for the nonlinear activations (see [40]). In input, a normalization is performed with a single linear transformation applied to pixel values (after the added noise if there is any), which results in inputs with approximate mean 0 and variance 1.

The heads  $\psi^i$  take as input the state representation (see Figure 1 and Figure 2), and are composed of 3 fully connected layers, the two first ones of size 24 and the last one of size 2, which corresponds to the size of the action vectors (1 torque per joint).

<sup>2</sup>The number of 24 dimensions has been selected empirically (not very large but leading to good RL results).

**SRLfD training details:** To learn a state representation, we run SRLfD (Algorithm 1) on the demonstration data for 2,000 epochs of approximately 1,000 steps, with batches of size  $b = 64$ .

**DDPG architecture:** We run DDPG with a policy network that has the same structure as the heads  $\psi^i$  used for imitation learning, but with rectified linear units (ReLU) for the activation functions. The number of parameters of the policy network depends on the size of its input, which is equal to the size of state representation. To prevent it from influencing the results simply because of the varying number of parameters, the inputs are repeated to form a vector of size close to 128, which yields policy networks with almost a constant number of parameters, no matter the size of the state representation in input.

**DDPG training details:** With every state representation, we run DDPG for 200 epochs consisting each of 20,000 training rollouts and 100 test rollouts.

## V. RESULTS

Figure 4 displays the mean learning curves obtained with different state representation methods in 4 different configurations: with a full representation of either 16 or 48 dimensions, and on raw observations or observations with noise and a randomly moving distractor. As expected, the best results are obtained with the ground truth representation, but we see that out of the 4 other state representations, only two can be successfully used by DDPG to solve reaching tasks when noise and a distractor are added to the inputs. These two methods are the PCA decomposition and SRLfD.

Figure 5 shows a detailed comparison between PCA and SRLfD for different sizes of the learned state representation (for inputs with noise and distractor). We observe that SRLfD state representations and PCA decompositions of large size lead to successful reinforcement learning. It is interesting to observe that reinforcement learning tends to perform increasingly better as the representation size increases, with all methods.<sup>3</sup> However, when we require the state representation to be compact (here, of dimension 24 or 16), SRLfD representations clearly outperform PCA decompositions.

PCA outperforms autoencoders in our study. It may seem counterintuitive as autoencoders are non-linear and can thus be expected to have a better performance. One possible explanation is that, as observed in the literature [4], [41], [42], they focus on the background and lose the important dynamic part, i.e. the robot arm, whereas the PCA is a linear method that cannot completely ignore this information.

## VI. CONCLUSION

We presented a method (SRLfD) for learning state representations from demonstrations, more specifically from runs of policies on different instances of tasks. Our results indicate that the state representations obtained can advantageously replace raw pixel inputs to learn policies on new task instances via

<sup>3</sup>Tests on much larger representations, however, show a decrease in performance at 128 dimensions, and at 4096 dimensions (equal to the observation size) the performance drops down to zero.



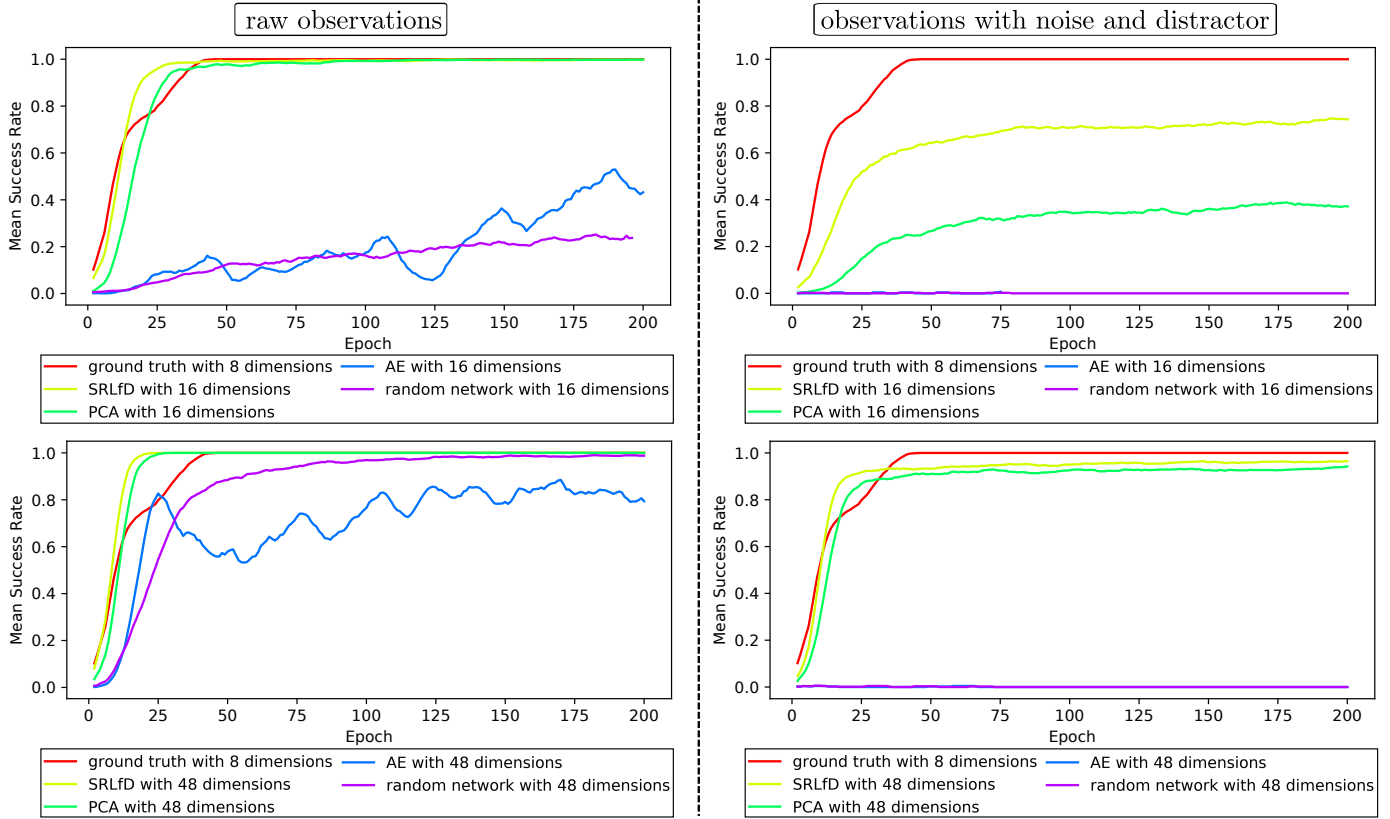


Fig. 4. RL with DDPG algorithm based on various state representations. The indicated dimensions correspond to the size of the state representation  $(\varphi, \Delta\varphi)$ . The learning curves are averaged over 8 executions: 4 learned representations (obtained with random seeds), and 2 runs of DDPG per representation, with a random position of the target goal for each run.

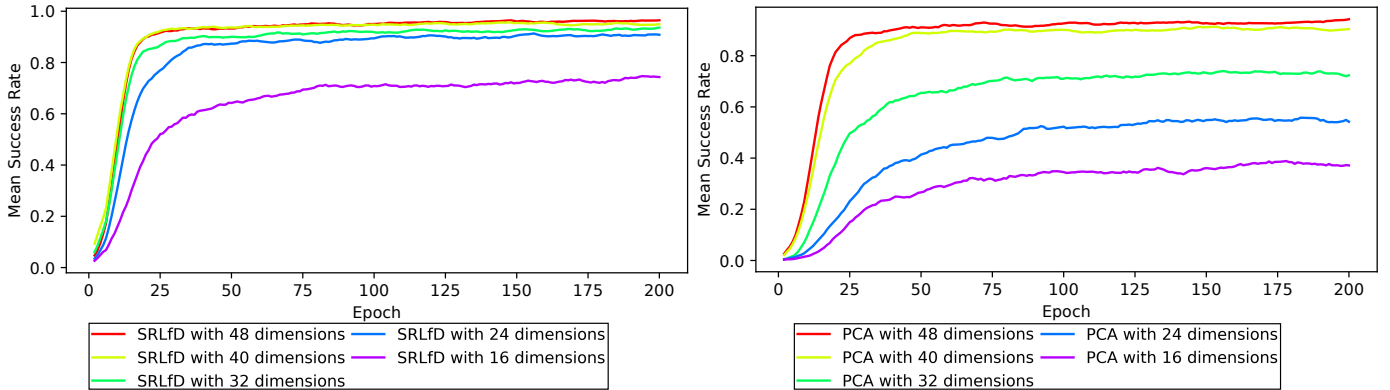


Fig. 5. Environment with noise and distractor. RL with DDPG algorithm based on SRLfD state representations (on the left) and PCA state representations (on the right). The indicated dimensions correspond to the size of the state representation  $(\varphi, \Delta\varphi)$ . As in Figure 4, the learning curves are averaged over 8 executions: 4 learned representations (obtained with random seeds), and 2 runs of DDPG per representation, with a random position of the target goal for each run.

end-to-end RL. By ensuring that the demonstration policies can be imitated with the learned state representation used as input, the proposed method forces the state representation to be general, provided that the demonstration policies are diverse. Moreover, since the representation is trained together with policies that imitate the demonstrations, we believe that it is likely to be more appropriate for control than other types of representations (for instance ones that primarily aim at enabling a good reconstruction of the raw inputs). The experimental results we obtained tend to confirm that belief,

as SRLfD state representations were more efficiently exploited by the DDPG reinforcement learning algorithm than 3 other types of state representations.

#### ACKNOWLEDGMENTS

This article has been supported within the Labex SMART supported by French state funds managed by the ANR within the Investissements d’Avenir programme under references ANR-11-LABX-65 and ANR-18-CE33-0005 HUSKI. We also gratefully acknowledge the support of NVIDIA Corporation with the donation of the Titan Xp GPU used for this research.

## REFERENCES

- [1] Y. Bengio, A. Courville, and P. Vincent, "Representation learning: A review and new perspectives," *IEEE transactions on pattern analysis and machine intelligence*, vol. 35, no. 8, pp. 1798–1828, 2013.
- [2] C. Olah, A. Mordvintsev, and L. Schubert, "Feature visualization," *Distill*, 2017, <https://distill.pub/2017/feature-visualization>.
- [3] Y. Bengio, "Deep learning of representations for unsupervised and transfer learning," in *Proceedings of ICML Workshop on Unsupervised and Transfer Learning*, 2012, pp. 17–36.
- [4] T. Lesort, N. Díaz-Rodríguez, J.-F. Goudou, and D. Filliat, "State representation learning for control: An overview," *arXiv preprint arXiv:1802.04181*, 2018.
- [5] C. Finn, X. Y. Tan, Y. Duan, T. Darrell, S. Levine, and P. Abbeel, "Deep spatial autoencoders for visuomotor learning," in *2015 IEEE International Conference on Robotics and Automation (ICRA)*. IEEE, 2015, pp. 512–519.
- [6] S. Levine, C. Finn, T. Darrell, and P. Abbeel, "End-to-end training of deep visuomotor policies," *The Journal of Machine Learning Research*, vol. 17, no. 1, pp. 1334–1373, 2016.
- [7] R. Jonschkowski and O. Brock, "Learning state representations with robotic priors," *Autonomous Robots*, vol. 39, no. 3, pp. 407–428, 2015.
- [8] B. D. Argall, S. Chernova, M. Veloso, and B. Browning, "A survey of robot learning from demonstration," *Robotics and autonomous systems*, vol. 57, no. 5, pp. 469–483, 2009.
- [9] L. C. Cobo, K. Subramanian, C. L. Isbell, A. D. Lanterman, and A. L. Thomaz, "Abstraction from demonstration for efficient reinforcement learning in high-dimensional domains," *Artificial Intelligence*, vol. 216, pp. 103–128, 2014.
- [10] C. Zhang, H. Zhang, and L. E. Parker, "Feature space decomposition for effective robot adaptation," in *Intelligent Robots and Systems (IROS), 2015 IEEE/RSJ International Conference on*. Citeseer, 2015, pp. 441–448.
- [11] T. P. Lillicrap, J. J. Hunt, A. Pritzel, N. Heess, T. Erez, Y. Tassa, D. Silver, and D. Wierstra, "Continuous control with deep reinforcement learning," *arXiv preprint arXiv:1509.02971*, 2015.
- [12] I. K. Fodor, "A survey of dimension reduction techniques," *Center for Applied Scientific Computing, Lawrence Livermore National Laboratory*, vol. 9, pp. 1–18, 2002.
- [13] W. Curran, T. Brys, M. Taylor, and W. Smart, "Using PCA to efficiently represent state spaces," *arXiv preprint arXiv:1505.00322*, 2015.
- [14] G. E. Hinton and R. R. Salakhutdinov, "Reducing the dimensionality of data with neural networks," *science*, vol. 313, no. 5786, pp. 504–507, 2006.
- [15] D. P. Kingma and M. Welling, "Auto-encoding variational bayes," *arXiv preprint arXiv:1312.6114*, 2013.
- [16] I. Higgins, L. Matthey, A. Pal, C. Burgess, X. Glorot, M. Botvinick, S. Mohamed, and A. Lerchner, "beta-vaes: Learning basic visual concepts with a constrained variational framework," in *International Conference on Learning Representations*, 2017.
- [17] M. Watter, J. Springenberg, J. Boedecker, and M. Riedmiller, "Embed to control: A locally linear latent dynamics model for control from raw images," in *Advances in neural information processing systems*, 2015, pp. 2746–2754.
- [18] J.-A. M. Assael, N. Wahlström, T. B. Schön, and M. P. Deisenroth, "Data-efficient learning of feedback policies from image pixels using deep dynamical models," *arXiv preprint arXiv:1510.02173*, 2015.
- [19] D. Ha and J. Schmidhuber, "World models," *arXiv preprint arXiv:1803.10122*, 2018.
- [20] R. Jonschkowski, R. Hafner, J. Scholz, and M. Riedmiller, "Pves: Position-velocity encoders for unsupervised learning of structured state representations," *arXiv preprint arXiv:1705.09805*, 2017.
- [21] P. Sermanet, C. Lynch, Y. Chebotar, J. Hsu, E. Jang, S. Schaal, and S. Levine, "Time-contrastive networks: Self-supervised learning from video," *arXiv preprint arXiv:1704.06888*, 2017.
- [22] R. Caruana, "Multitask learning," *Machine learning*, vol. 28, no. 1, pp. 41–75, 1997.
- [23] M. E. Taylor and P. Stone, "Transfer learning for reinforcement learning domains: A survey," *Journal of Machine Learning Research*, vol. 10, no. Jul, pp. 1633–1685, 2009.
- [24] L. Pinto and A. Gupta, "Learning to push by grasping: Using multiple tasks for effective learning," in *Robotics and Automation (ICRA), 2017 IEEE International Conference on*. IEEE, 2017, pp. 2161–2168.
- [25] A. A. Rusu, S. G. Colmenarejo, C. Gulcehre, G. Desjardins, J. Kirkpatrick, R. Pascanu, V. Mnih, K. Kavukcuoglu, and R. Hadsell, "Policy distillation," *arXiv preprint arXiv:1511.06295*, 2015.
- [26] E. Shelhamer, P. Mahmoudieh, M. Argus, and T. Darrell, "Loss is its own reward: Self-supervision for reinforcement learning," *arXiv preprint arXiv:1612.07307*, 2017.
- [27] C. Finn, P. Abbeel, and S. Levine, "Model-agnostic meta-learning for fast adaptation of deep networks," *arXiv preprint arXiv:1703.03400*, 2017.
- [28] C. Devin, A. Gupta, T. Darrell, P. Abbeel, and S. Levine, "Learning modular neural network policies for multi-task and multi-robot transfer," in *Robotics and Automation (ICRA), 2017 IEEE International Conference on*. IEEE, 2017, pp. 2169–2176.
- [29] P. Pastor, H. Hoffmann, T. Asfour, and S. Schaal, "Learning and generalization of motor skills by learning from demonstration," in *Robotics and Automation, 2009. ICRA'09. IEEE International Conference on*. IEEE, 2009, pp. 763–768.
- [30] J. Kober, A. Wilhelm, E. Oztop, and J. Peters, "Reinforcement learning to adjust parametrized motor primitives to new situations," *Autonomous Robots*, vol. 33, no. 4, pp. 361–379, 2012.
- [31] C. Finn, T. Yu, T. Zhang, P. Abbeel, and S. Levine, "One-shot visual imitation learning via meta-learning," *arXiv preprint arXiv:1709.04905*, 2017.
- [32] M. Večerík, T. Hester, J. Scholz, F. Wang, O. Pietquin, B. Piot, N. Heess, T. Rothörl, T. Lampe, and M. Riedmiller, "Leveraging demonstrations for deep reinforcement learning on robotics problems with sparse rewards," *arXiv preprint arXiv:1707.08817*, 2017.
- [33] A. Nair, B. McGrew, M. Andrychowicz, W. Zaremba, and P. Abbeel, "Overcoming exploration in reinforcement learning with demonstrations," in *2018 IEEE International Conference on Robotics and Automation (ICRA)*. IEEE, 2018, pp. 6292–6299.
- [34] Y. Tassa, Y. Doron, A. Muldal, T. Erez, Y. Li, D. d. L. Casas, D. Budden, A. Abdolmaleki, J. Merel, A. Lefrancq, *et al.*, "Deepmind control suite," *arXiv preprint arXiv:1801.00690*, 2018.
- [35] E. Todorov, T. Erez, and Y. Tassa, "Mujoco: A physics engine for model-based control," in *Intelligent Robots and Systems (IROS), 2012 IEEE/RSJ International Conference on*. IEEE, 2012, pp. 5026–5033.
- [36] M. Andrychowicz, F. Wolski, A. Ray, J. Schneider, R. Fong, P. Welinder, B. McGrew, J. Tobin, O. P. Abbeel, and W. Zaremba, "Hindsight experience replay," in *Advances in Neural Information Processing Systems*, 2017, pp. 5048–5058.
- [37] I. Jolliffe, "Principal component analysis," in *International encyclopedia of statistical science*. Springer, 2011, pp. 1094–1096.
- [38] V. Dumoulin and F. Visin, "A guide to convolution arithmetic for deep learning," *arXiv preprint arXiv:1603.07285*, 2016.
- [39] A. Gaier and D. Ha, "Weight agnostic neural networks," *arXiv preprint arXiv:1906.04358*, 2019.
- [40] Y. A. LeCun, L. Bottou, G. B. Orr, and K.-R. Müller, "Efficient backprop," in *Neural networks: Tricks of the trade*. Springer, 2012, pp. 9–48.
- [41] T. de Bruin, J. Kober, K. Tuyls, and R. Babuška, "Integrating state representation learning into deep reinforcement learning," *IEEE Robotics and Automation Letters*, vol. 3, no. 3, pp. 1394–1401, 2018.
- [42] A. Raffin, A. Hill, R. Traoré, T. Lesort, N. Díaz-Rodríguez, and D. Filliat, "S-rl toolbox: Environments, datasets and evaluation metrics for state representation learning," *arXiv preprint arXiv:1809.09369*, 2018.